Presented at the International
Colloquium on Drops and Bubbles,
Pasadena, CA, Aug. 28-30, 1974

LBL-3363
c.2

THE ROTATING, CHARGED OR GRAVITATING LIQUID DROP, AND PROBLEMS IN NUCLEAR PHYSICS AND ASTRONOMY

W. J. Swiatecki

August 1974

Prepared for the U.S. Atomic Energy Commission
under Contract W-7405-ENG-48

TWO-WEEK LOAN COPY

This is a Library Circulating Copy which may be borrowed for two weeks. For a personal retention copy, call Tech. Info. Division, Ext. 5545

LAWRENCE BERKELEY LABORATORY
UNIVERSITY OF CALIFORNIA
BERKELEY

LBL-3363
c.2

DISCLAIMER

This document was prepared as an account of work sponsored by the United States Government. While this document is believed to contain correct information, neither the United States Government nor any agency thereof, nor the Regents of the University of California, nor any of their employees, makes any warranty, express or implied, or assumes any legal responsibility for the accuracy, completeness, or usefulness of any information, apparatus, product, or process disclosed, or represents that its use would not infringe privately owned rights. Reference herein to any specific commercial product, process, or service by its trade name, trademark, manufacturer, or otherwise, does not necessarily constitute or imply its endorsement, recommendation, or favoring by the United States Government or any agency thereof, or the Regents of the University of California. The views and opinions of authors expressed herein do not necessarily state or reflect those of the United States Government or any agency thereof or the Regents of the University of California.

THE ROTATING, CHARGED OR GRAVITATING LIQUID DROP, AND PROBLEMS IN NUCLEAR PHYSICS AND ASTRONOMY*

W. J. Swiatecki
Lawrence Berkeley Laboratory, University of California, Berkeley, CA 94720

ABSTRACT

A survey is presented of the equilibrium configurations of a rotating charged or gravitating liquid mass in a way that unifies the treatment of idealized rotating heavenly bodies, rotating drops in a weightless environment, and idealized rotating nuclei. A number of applications, especially to nuclear physics, is described.

I. INTRODUCTION

Figure 1 is a photograph of the planet Jupiter. The slightly flattened appearance is caused by rotation.

Figure 2 is a glass droplet from the lunar soil returned by the Apollo 11 mission (length about 1 mm). Presumably it was ejected from a meteorite impact on the moon as a molten, rotating blob, which solidified in flight.

Figure 3 is a picture of a series of sketches made by Niels Bohr on November 7, 1950 (his 65th birthday), during a conversation on the liquid drop theory of nuclear fission. On the right is a sequence of shapes of a fissioning nucleus of Np^{237}, calculated in 1968 by J. R. Nix using that theory. (Ref. 1)

These figures illustrate three fields in which the theory of rotating, charged or gravitating masses has found an application: astronomy, hydrodynamics in a weightless environment and nuclear physics.

Historically the theory of rotating homogeneous masses as idealized representations of planets, stars and nebulae goes back to Newton's investigations on the figure of the earth. In the past two and a half centuries the theory has been developed by many illustrious mathematicians, among them Maclaurin, Jacobi, Riemann, Poincaré, Liapunov, Jeans, Darwin, Cartan, Appell, and Lyttelton. In the last decade the subject was taken up anew by S. Chandrasekhar and N. Lebovitz and brought to a rare degree of perfection in Chandrasekhar's monumental work on "Ellipsoidal Figures of Equilibrium." (Ref. 2)

The theory of a rotating liquid mass endowed with a surface tension but no gravitational forces was stimulated by Plateau's experiments 100 years ago with globes of oil suspended in a liquid of the same density. The experiments were discussed in connection with Laplace's nebular hypothesis of the origin of the solar system. An account of the earlier investigations is given in Appell's "Mécanique Rationnelle". (Ref. 3, Vol. 4, Ch. IX)

The theory of rotating liquid masses with a surface tension and a uniform electric charge arose in nuclear physics in connection with the

study of nuclei endowed with large angular momenta. The major part of the binding energy of a nucleus is well represented by the model of a uniformly charged liquid drop with a surface tension, and the addition of a rotational energy to the conventional volume, surface, and electrostatic energies of the liquid drop model constitutes an interesting generalization. A number of authors, among them Pik-Pichak, Beringer and Knox, Hiskes, Sperber, Carlson and Pau Lu, Cohen, Plasil and Swiatecki, Chandrasekhar, Rosenkilde, Mollenauer and Wheeler have addressed themselves to this problem in the past 15 years. (See list of references in Ref. 4.)

It was soon realized that the astronomical problem, Plateau's problem and the nuclear problem are formally special cases of a single mathematical structure. They can in fact be discussed in a unified way by varying continuously a single parameter in the equations, the parameter being the relative intensity of the inverse-distance (gravitational or electrostatic) energy. In this way a problem of irresistible scope presents itself: to discuss in a unified manner the equilibrium shapes of rotating masses representing at one extreme idealized atomic nuclei, at the other idealized heavenly bodies, and covering in between engineering applications in weightless space laboratories. In this talk I would like to give you a survey of the problem from this unified point of view.

2. STATEMENT OF THE PROBLEM

Let me first state the idealized mathematical problem precisely. We consider a given volume of an incompressible fluid with a sharp boundary (which may or may not be simply connected--it may be in two or more pieces). The fluid may be gravitating and/or uniformly charged, it is endowed with a surface tension, and is rotating with a given angular momentum about its center of mass. The question is: what are the shapes of gyrostatic equilibrium of the fluid, i.e., shapes in which the only motion of all fluid elements is a uniform rotation with a common angular velocity?

The way one answers such a problem in gyrostatics is by writing down an effective potential energy and making it stationary with respect to all infinitesimal variations of the fluid boundary. This effective potential energy E is the ordinary potential energy augmented by a rotational energy. Thus in our case

$$E = E_S + E_I + E_R \quad . \tag{1}$$

Here E_S is the surface energy, equal to the surface area of the configuration in question times the surface energy coefficient γ:

$$E_S = \gamma \oint d\sigma \quad .$$

The quantity E_I is the inverse-distance energy, the sum of interactions between pairs of volume elements $d\tau_1$ and $d\tau_2$ interacting according to an inverse-distance potential:

$$E_I = (\rho_e^{\,2} - G\rho^2)\,\frac{1}{2}\iiiint\!\!\iint \frac{d\tau_1\, d\tau_2}{r_{12}} \quad .$$

Here ρ_e is the uniform density of electric charge, ρ is the mass density and G is the constant of gravitation. (In most cases of practical interest one of the two quantities $\rho_e^{\,2}$, $G\rho^2$ is negligible compared to the other.)

The rotational energy is the square of the angular momentum L divided by twice the moment of inertia of the configuration in question:

$$E_R = L^2 \Big/ 2\rho \iiint r_\perp^{\,2}\, d\tau \ . \tag{1a}$$

Here $r_\perp$ is the perpendicular distance of the volume element $d\tau$ from the axis of rotation (passing through the center of mass of the whole system).

For a spherical configuration with radius R these energies reduce to

$$E_S^{(0)} = 4\pi R^2\,\gamma$$

$$E_I^{(0)} = \frac{3}{5}(Q^2 - GM^2)\,\frac{1}{R} \ ,$$

$$E_R^{(0)} = \frac{1}{2}\cdot\frac{L^2}{\frac{2}{5}MR^2} \ ,$$

where Q is the total charge and M the total mass of the system. The above energies provide convenient units in which to express the three quantities E_S, E_I, E_R, and we may then rewrite the effective potential energy in a dimensionless way that is especially suited for a unified discussion of the problem. Picking $E_S^{(0)}$ as the unit for the effective potential energy we may write

$$\varepsilon \equiv \frac{E}{E_S^{(0)}} = \Phi_S + \frac{E_I^{(0)}}{E_S^{(0)}}\,\Phi_I + \frac{E_R^{(0)}}{E_S^{(0)}}\,\Phi_R \ . \tag{2}$$

Here Φ_S, a function of the shape of the configuration in question, is the surface energy in units of the surface energy of the spherical shape. (Thus Φ_S(sphere) = 1.) Similarly Φ_I is the inverse-distance energy in units of its value for the sphere, and Φ_R is the rotational energy, given by Eq. (1a), in units of what it would be for a sphere.

This way of writing the energy brings out the fact that since there are three energies in the problem (surface, inverse distance, rotational) there are two dimensionless ratios, which may be taken as the parameters of the unified theory. These ratios are often denoted by x and y, and defined as follows:

$$x \equiv \frac{1}{2}\frac{E_I^{(0)}}{E_S^{(0)}} = \frac{(\text{Charge})^2 - G(\text{Mass})^2}{10(\text{Volume})(\text{Surface Tension Coeff.})} \tag{3a}$$

$$y \equiv \frac{E_R^{(0)}}{E_S^{(0)}} = \frac{5}{12}\frac{(\text{Angular Momentum})^2}{(\text{Volume})(\text{Mass})(\text{Radius})(\text{Surface Tension Coeff.})} \; . \tag{3b}$$

The parameter y is a measure of the square of the angular momentum, and thus of the size of the disruptive centrifugal forces compared to the cohesive surface tension forces. When GM^2 is negligible the parameter x reduces to the conventional 'fissility parameter' of nuclear physics, a measure of the disruptive electrostatic forces compared to the surface tension forces.

The dimensionless effective potential energy now reads

$$\varepsilon = \Phi_S(\text{Shape}) + + 2x\,\Phi_I(\text{Shape}) + y\,\Phi_R(\text{Shape}) \; . \tag{4}$$

The Φ's are dimensionless functions of the shape only. For example, for spheroidal shapes specified by semi-axes a,c (where c is along the axis of symmetry) one finds the following formulae in terms of the eccentricity e (equal to $\sqrt{1 - a^2/c^2}$):

$$\Phi_S = \frac{1}{2}(1 - e^2)^{1/3}\left[1 + \frac{\sin^{-1} e}{e(1 - e^2)^{1/2}}\right] \tag{5a}$$

$$\Phi_I = \frac{1}{2}(1 - e^2)^{1/3}\,\frac{1}{e}\,\ln\frac{1 + e}{1 - e} \tag{5b}$$

$$\Phi_R = \frac{1}{2}(1 - e^2)^{-2/3}(2 - e^2) \; . \tag{5c}$$

For configurations specified by several shape parameters the Φ's are functions of several variables. In any case the important thing is that the Φ's can be calculated and tabulated once and for all, independently of the

particular physical system that is being investigated. Imagine that such a tabulation of the Φ's has been carried out. Then to find the configurations of gyrostatic equilibrium for a given system we first calculate the values of x and y that specify that system (using Eqs. 3a, 3b), insert these in Eq. (4), and vary the shape until ε is stationary. For a different system we will have another pair of x,y values. To cover all possible systems we would vary both x and y in the full range from $-\infty$ to $+\infty$ and file away the results in a two-parameter filing cabinet illustrated in Fig. 4. This figure brings out the relations to one another of various physical systems. To orient ourselves: $y = 0$ means no rotation, so along the positive x-axis we have the domain of nonrotating idealized nuclei, from light to heavy with increasing x. For negative x we have gravitating globes. The classic case of astronomical masses for which surface tension is negligible corresponds to $x \to -\infty$, indicated on the left. Plateaus rotating globes, with no charge and negligible gravitation, correspond to the positive y-axis. Rotating nuclei and rotating gravitating masses with surface tension fill the upper half-plane.

What about negative values of y? At first this sounds silly (a negative centrifugal force--an imaginary angular momentum?). In fact, however, systems with negative y-values are quite possible. Thus the negative y-axis corresponds to a bubble in a rotating container filled with a liquid. The bubble is an object with negative intertial mass relative to the surrounding liquid, and experiences a negative centrifugal force which, instead of flattening the bubble tends to elongate it along the axis of rotation. (Similarly a bubble in a container filled with gravitating matter belongs in the lower right-hand quadrant and a bubble in rotating, uniformly charged nuclear matter belongs in the lower left-hand quadrant.)

So now we have a filing system in which results on idealized stars and planets, weightless globes, idealized nuclei and bubbles may be displayed in a unified way. Let us remind ourselves what it is that we will be displaying in the filing cabinet. Take a rotating system with a given value of x,y. You might think at first that there will be just one entry, the equilibrium shape of that system. In fact there will be several entries because a given system with a given angular momentum has, in general, many configurations of equilibrium. Thus the effective potential energy for a given system, plotted as a function of, say, two shape degrees of freedom, might look something like Fig. 5. This shows a metastable minimum A, as well as an absolute minimum C, separated by a saddle-point B. Off to the side there is a mountain top D. All such points A, B, C, D are equilibrium shapes, although only some are stable whilst others are unstable, with different degrees of instability. Some of the unstable shapes are of great interest--for example a saddle-point shape of the type B is of crucial importance in the theory of nuclear fission and must be calculated in order to estimate fission barrier heights and spontaneous fission lifetimes of nuclei in situations of practical relevance.

Here let me make an important qualification of the words stable and unstable. In Fig. 5 one would be tempted to call A and B stable and C and D unstable configurations of equilibrium. For truly static, nonrotating systems ($y = 0$) that is indeed the case and that's all there is to it. But for gyrostatic systems it is not so, and it is possible--sometimes--

to have a system oscillating around a mountain top with bounded oscillations--rather than sliding down. This is an effect of coriolis (gyroscopic) forces, which are not contained in the effective potential energy E: the effective potential energy does not have in it the information about the full dynamical problem. This makes it obviously extremely dangerous to jump to conclusions about the stability or instability of the dynamical motion on the basis of the appearance of the effective potential energy landscape. There is, however, a mitigating circumstance which partly restores to the effective potential energy its role as a guide to the stability or instability of equilibrium points. Thus if there are dissipative effects present in the system (friction, viscosity), then, if one waits long enough so that these effects can assert themselves, saddles and mountain tops will, after all, behave in an unstable way, as one would have expected to begin with. This kind of instability, which requires that you wait long enough for dissipation to assert itself, is called secular instability.

In what follows when I say 'unstable' I shall always mean 'secularly unstable'.

Coming back to our x-y filing cabinet we see that the full problem of discussing the shapes of gyrostatic equilibrium of rotating masses consists of calculating all the important shapes, stable and unstable, for a given pair of x,y values, and then tracing out the behavior of these shapes as functions of x and y in the full x-y plane.

How much of this complete picture is known today? I will try to give you an impression of that in my talk, but let me say at once that the problem has been only partly explored, and there remains a beautiful project for mathematicians, physicists and astronomers to work on.

Let me first give you a bare-bones summary of what happens in various regions of the x-y plane, and then let me fill in some of the details.

3. SUMMARY OF STABILITY REGIONS

By piecing together old results in the three familiar regions in the x-y plane (astronomical masses, Plateau globes, nonrotating nuclei) and adding calculations and estimates in the other portions, one arrives at the following picture, summarized in Fig. 6.

For small amounts of rotation the originally spherical drop is flattened by the centrifugal force into an oblate spheroid, independently of the value of x, i.e., independently of whether we discuss a gravitating liquid mass with or without surface tension, or a charged nuclear droplet. For finite values of y the equilibrium configurations are no longer exact spheroids and we shall refer to these shapes as pseudospheroids or Hiskes shapes. In the astronomical limit of zero surface tension the oblate shapes of equilibrium do happen to be exact spheroids: they are the Maclaurin spheroids. The spheroids or pseudospheroids continue to flatten with increasing rotation and they remain stable until a certain critical value of y, denoted by y_I, which is a function of x. (Fig. 6) At this point the pseudospheroids become secularly unstable and a qualitative change takes place. The nature of the change depends on whether x is below or above a certain critical value x_c,

which is today not yet determined exactly, but appears to be in the neighborhood of $x_c = 0.81$. This corresponds to heavy nuclei towards the end of the periodic table.

If $x > x_c$ the flat pseudospheroids become secularly unstable towards disintegration, by way of a triaxial deformation.

If $x < x_c$, and this includes the rest of the periodic table as well as uncharged droplets, molten asteroids and astronomical gravitating masses, the flat pseudospheroid becomes secularly unstable towards conversion into a nonaxially symmetric configuration of equilibrium, which branches off the pseudospheroids at the critical value y_I. This new configuration has the symmetry of an ellipsoid with three unequal axes and rotates about its shortest axis. The other two axes are at first almost equal (when y exceeds the critical value by an infinitesimal amount and the equilibrium configuration is almost axially symmetric). Later these two axes become rapidly unequal, one of them becoming longer and longer as y increases, and the other tending to approximate equality with the shortest axis about which the rotation is taking place. The general appearance of these configurations is that of flattened cylinders with rounded ends and a somewhat elliptic cross section. In the astronomical limit of large negative x these configurations are exact ellipsoids (the Jacobi ellipsoids): otherwise the tips of the figure are more rounded. For certain values of x (in the neighborhood of 0) there is even a suggestion of a dumb-bell or hourglass shape. We shall refer to these configurations as pseudo-ellipsoids, or as Beringer-Knox shapes.

As the angular momentum is increased beyond the first critical value y_I the pseudo-ellipsoids which exist for $x < x_c$ become more and more elongated under the influence of the centrifugal force until a second critical value of y is reached, denoted by y_{II}. At this value of y the family of triaxial pseudo-ellipsoids comes to an end by way of loss of equilibrium towards a reflection symmetric disintegration mode. If x is greater than a second critical value of x, denoted by x_{cc} (and equal to about -0.4), the pseudo-ellipsoids are stable shapes up to the critical value y_{II}, when they cease to exist. If, however, $x < x_{cc}$, the pseudo-ellipsoids lose stability against a reflection asymmetric disintegration mode along the critical curve denoted by y_{III} in Fig. 6. This occurs before the disappearance of the pseudo-ellipsoids at y_{II}, so that in the case of $x < x_{cc}$ the pseudo-ellipsoids exist but are unstable against asymmetry in the region between y_{III} and y_{II}.

We may summarize the situation as follows: A sufficient amount of rotation will always disintegrate a fluid mass, be it gravitating or charged. The critical amount of rotation is, naturally, a decreasing function of x, being given by the curve $y_I(x)$ for $0.81 \lesssim x < 1$, by $y_{II}(x)$ for $-0.4 \lesssim x \lesssim 0.81$ and by $y_{III}(x)$ for $-\infty < x \lesssim -0.4$.

The disintegration occurs by way of a <u>loss of stability</u> against a triaxial mode in the first case, by way of a <u>loss of equilibrium</u> against a reflection symmetric mode in the second case, and by way of <u>loss of stability</u> against a reflection asymmetric mode in the third case. Note the distinction

between loss of stability and loss of equilibrium. Loss of stability in a family of equilibrium shapes means that for a parameter (e.g., y) in excess of a critical value an equilibrium shape exists but has changed from stable to unstable, i.e., the second derivative of the energy has changed sign. Loss of equilibrium means that the family of equilibrium shapes has ceased to exist: with the parameter in excess of the critical value the condition for equilibrium, $\delta E = 0$, cannot be satisfied, i.e., the condition of the vanishing of the first derivative of the energy has no (real) solutions. As noted before, when we say "unstable" we mean "secularly unstable".

Finally a note about the astronomical limit $x = -\infty$, or $x^{-1} = 0$. The situation is similar to the case of $-\infty < x < x_{cc}$ in that increasing angular momentum leads to a loss of stability against a reflection asymmetric mode. Nevertheless the case of zero surface tension ($x^{-1} = 0$) is a special case, different from the case of a finite surface tension, however small, in that for $x^{-1} = 0$ the Jacobi ellipsoids are shapes of equilibrium for any value of y, even exceeding y_{II}. In this (astronomical) case y_{II} does not mark the end of the ellipsoids (a loss of equilibrium) but merely a loss of stability against a reflection symmetric disintegration mode. More about this later.

Now let me amplify this summary by discussing more fully various regions in the x-y diagram.

4. NONROTATING NUCLEI, $y = 0$, $x > 0$

Let me start with the simplest example, the case of a nonrotating idealized nucleus. If one is asked what are the configurations of equilibrium of a nonrotating, uniformly charged drop, the obvious answer is: a sphere. A sphere is a shape of equilibrium for any amount of charge on the drop, i.e., for any value of x. This isn't the complete answer, however, since n equal spherical fragments dispersed to infinity are also equilibrium configurations. It follows that in the many-dimensional configuration space of the system there will be many potential energy hollows, one for each n. (You may verify trivially from the definitions of Φ_S and Φ_I that for n equal fragments at infinity $\Phi_S = n^{1/3}$, $\Phi_I = n^{-2/3}$, so the energy of the nth potential energy hollow is given by

$$\varepsilon = n^{1/3} + 2x\, n^{-2/3} .$$

This simple equation tells interesting things about the relative depths of the hollows. For example one learns the important fact that the absolute minimum (the lowest hollow) for any given x is the one corresponding to approximately $n \approx 4x$.

The realization that the potential-energy landscape has many hollows leads to an important discovery. Thus it is a simple topological requirement that if you have several hollows in a landscape then there must be saddle-point passes between them. The simplest case is a one-dimensional landscape: if a continuous curve has two minima there must be a maximum--a barrier--between them. (Essentially Rolle's theorem.) For example let us focus attention on a sequence of deformations leading from a single charged spherical drop to two equal fragments at infininte separation. Figure 7

indicates how the two minima must be separated by a maximum, corresponding to the so-called Bohr-Wheeler saddle-point shape for nuclear fission. To be specific, the configuration of a Lead nucleus at the Bohr-Wheeler saddle point is a somewhat necked-in cylinder with rounded ends--a little like an hour-glass figure with two equal bulbs. The energy of this shape is a maximum with respect to the division coordinate, but a minimum with respect to other shape coordinates (e.g., an asymmetry coordinate, which changes the relative sizes of the two bulbs of the hour-glass figure). Figure 7 illustrates further that even though the saddle shape is stable with respect to small changes in the relative sizes of the bulbs, a sufficiently large asymmetry makes the energy decrease again, after passage over a mountain top. The mountain-top configuration of a nucleus--an asymmetric hour-glass figure with unequal bulbs--is called the Businaro-Gallone shape and is of importance for the question of "fission asymmetry"--i.e., whether an idealized nucleus would divide into equal or unequal pieces. Thus a central problem in the early years of the theory of nuclear fission was, first, the tracing out of the Bohr-Wheeler saddle-point shape (and the associated barrier height) as a function of the fissility parameter x and, second, the tracing out of the Businaro-Gallone mountain tops. Many authors have contributed to the solution of this problem. Figure 8 shows some calculations of saddle-point shapes from Ref. 5. The shapes range from tangent spheres for $x = 0$, through hour-glass figures, to spheroids and finally a sphere at $x = 1$. As x tends to 1 and the saddle shape approaches the sphere the height of the potential energy barrier against fission decreases and finally vanishes at $x = 1$. This is illustrated in Fig. 9, taken from Ref. 1. You may veryify by using Eqs. (5a) and (5b), expanded to the leading power of the eccentricity, that the loss of stability of a charged sphere does indeed occur at $x = 1$. With a little more trouble, by expanding to the next power in e^2, you may also calculate from these expressions that the barrier height for fission, in units of $E_S^{(0)}$, is given by

$$\frac{\text{Barrier}}{E_S^{(0)}} = \frac{98}{135}(1 - x)^3 + \text{higher powers of } (1 - x) \quad . \qquad (6)$$

When $1 - x$ is not small this formula is not applicable and numerical methods have to be resorted to in order to calculate the barrier heights in their dependence on x. Numerical methods, using digital computers, were also necessary to trace out the behavior of the Businaro-Gallone mountain tops, and to establish the important result that they exist only if x is greater than 0.396. (A consequence of this is that the Bohr-Wheeler saddle shapes are stable against reflection asymmetric deformations for $x > 0.396$ and unstable for $x < 0.396$.)

It would be too cumbersome for me to display all these symmetric and asymmetric shapes in detail, so let me show you a condensed summary of the behavior of the Bohr-Wheeler and Businaro-Gallone equilibrium shapes as functions of x.

Figure 10 shows just the major and minor semi-axes, essentially the tip-to-center-of-mass distance and the neck radius of these elongated figures. In the upper part of the figure you see the major semiaxis of the Bohr-Wheeler shape as it increases at first with increasing x and then, rather suddenly, begins to decrease around $x \approx 2/3$, finally tending

to 1 (the sphere) at $x = 1$. The Businaro-Gallone shapes, being reflection asymmetric, have two unequal tip distances, indicated by the dashed curve which branches off (bifurcates from) the solid curve at $x = 0.396$. The lower part of the figure shows the behavior of the neck radius.

Through such numerical studies the properties of the Bohr-Wheeler shapes are now known adequately. But the story of the Businaro-Gallone dumbbells is not completely cleared up even today. It is only relatively recently that one realized that they probably disappear again for x greater than about 0.8, so we have the peculiar result that a charged drop possesses a Businaro-Gallone asymmetric shape of (unstable) equilibrium only if its fissility parameter is between about 0.4 and 0.8 (in round numbers).

Let me now give you a few examples of the relevance of this theory of the equilibrium shapes of an idealized charged liquid drop to nuclear physics. To begin with, Fig. 11 illustrates how the sum of a volume energy, a surface energy and an electrostatic energy of the stable spherical equilibrium configuration of an idealized liquid drop reproduces the principal features of the nuclear binding energies. (The quantity plotted in Fig. 11 is the "mass decrement", closely related to the nuclear binding energy.) The curve is a liquid drop model fit to the experimental data. The deviations, up to ~ 12 MeV, are caused by nuclear "shell effects", which set a limit to the applicability of the liquid drop model. The total binding energy of a heavy nucleus is almost 2000 MeV, so on a gross scale the fit is satisfactory. On a finer scale one has to worry about the shell-effect deviations. This is illustrated in the lower part of Fig. 12, where the deviations from the liquid-drop model fit to nuclear masses are shown for some heavy nuclei. The largest deviation is at the "doubly magic" nucleus Pb^{208}, where the shells at $N = 126$ and $Z = 82$ give an additional binding of some 12 MeV.

The upper part of Fig. 12 compares the experimental and calculated masses for the same set of nuclei, but when their shapes are the deformed Bohr-Wheeler configurations instead of the near-spherical ground states. As expected (from the theory of shell effects) the deformation seems to have destroyed the extra shell-effect binding, and the liquid drop theory now reproduces the masses to within a couple of MeV. The increase of the saddle-point masses with decreasing x is essentially that predicted by the barrier formula, Eq. (6).

It is from such fits to nuclear ground state and saddle-point masses that one estimates that the surface energy coefficient of nuclei is about 1 MeV/fm^2 or, equivalently, that the surface energy of a nucleus with mass number A is about (18 MeV)$A^{2/3}$. Knowing this fact we may calculate the fissility parameter of a nucleus with mass number A and charge Ze as follows:

$$E_I^{(0)} = \frac{3}{5}\frac{(Ze)^2}{R}$$ (the electrostatic energy of a uniformly charged sphere of radius R)

$$E_S^{(0)} = 18\ A^{2/3}\ \text{MeV}.$$

Remembering that $R \approx 1.2\ A^{1/3}$ fm and $e^2 = 1.44$ MeV fm (1 fm = 10^{-13} cm) we find

$$x = \frac{E_I^{(0)}}{2E_S^{(0)}} \approx \frac{1}{50}\frac{Z^2}{A} \quad \text{in round numbers.}$$

As we saw, the barrier against nuclear fission vanishes at $x = 1$, which we can now translate into the statement that $(Z^2/A) \lesssim 50$ for stability against fission. This is a most fundamental prediction of the liquid drop theory of nuclei, for it provides an interpretation of the termination of the periodic system of chemical elements somewhere in the vicinity of atomic number 100. The basic reason why there are only some 100 elements found in nature is that (even after stability against alpha and beta decay has been assured) the intensity of electrification for heavier nuclei begins to violate the liquid drop stability criterion $x < 1$.

I have given you only a few specific examples of the application of the liquid drop theory to nuclei. To get a broader perspective let me say that in the last 10 years we have learned how to calculate the potential energies of nuclei, in their dependence on N, Z and the nuclear shape, with an accuracy of about 1 in 1000. This has been possible in virtue of a two-part approach, where shell corrections of about 10 MeV are added to a smooth background of hundreds of MeV. This smooth background, an indispensable part of the nuclear energy, is provided by the model of a charged liquid drop.

5. ROTATING NUCLEI AND THE PLATEAU CASE, $x \geqslant 0$, $y > 0$

If an uncharged globe with surface tension is rotated, it flattens at first into an oblate pseudospheroid which, with increasing angular momentum (increasing y), eventually goes over into a torus. (See Fig. 13.) Well before this happens, at the critical value y_I equal to 0.2829, the oblate shape becomes secularly unstable towards conversion into a triaxial pseudo-ellipsoid rotating about its shortest axis, analogous to the Jacobi ellipsoid. In contrast to the Jacobi ellipsoids, the family of pseudo-ellipsoids comes to an end at the critical value y_{II}, equal approximately to 0.785 for $x = 0$. (See Fig. 6.) For uniformly charged (nuclear) drops the critical values y_I and y_{II} decrease with x. Figure 14 gives some details of the case $x = 0.3$, corresponding to nuclei in the general vicinity of atomic numbers $Z \approx 35$. The major semiaxis R_{max}/R for the pseudo-spheroidal (Hiskes) shapes increases gradually with y. At $y = 0.18$ the pseudo-ellipsoidal (Beringer-Knox) shapes bifurcate. The curve for the semimajor axis of this family continues to increase with y up to the critical turning point y_{II}, where it goes around a bend. After the bend the curve describes the semimajor axis of the triaxial saddle-point shape (the Pik-Pichak saddle) for fission. This shape is the generalization to the case with angular momentum of the hour-glass Bohr-Wheeler saddle. The $y = 0$ member of this family of Pik-Pichak saddles is in fact a Bohr-Wheeler shape.

Figure 15 gives an indication of the actual appearance of these shapes For example, in the upper right-hand part the sphere labeled H (for Hiskes)

is the equilibrium shape and the hour-glass figure PP (for Pik-Pichak) is the saddle-point shape for $y = 0$. At $y = 0.16$ the Hiskes shape has flattened into a pseudo-spheroid and the neck of the Pik-Pichak shape has thickened. At $y = 0.24$ the stable ground state is now a Beringer-Knox psuedo-ellipsoid. For $y = 0.4$ the Beringer-Knox shape shows some necking and is about to coalesce with the Pik-Pichak saddle shape. All the Beringer-Knox shapes and all the Pik-Pichak shapes (except the one for $y = 0$) are slightly triaxial. In the figure only the mean section of these triaxial shapes is indicated.

A practical application of these calculations is the prediction of the existence of "super-deformed" nuclei, elongated into cylinder-like shapes with a ratio of axes of about 2:1 by the centrifugal forces arising from the collision of two nuclei. As an example the bombardment of a Si target with Ar ions of about 170 MeV energy might lead in a fraction of the collisions to super-deformed compound nuclei.

The discovery of such nuclei, stretched out by the centrifugal force into triaxial shapes, so closely analogous to the classic Jacobi ellipsoids, would be an exciting event. So far insufficient effort has been devoted to the identification of such nuclei and they have not been seen experimentally.

6. ASTRONOMICAL LIMIT $x \to -\infty$, $y > 0$

Let me now review the left-hand edge of our filing cabinet: the classic problem of a rotating gravitating mass (without surface tension).

First a small change in notation. Since there is now no surface energy the ratio of $E_R^{(0)}$ to the gravitational energy of a sphere is a natural parameter. Thus we introduce

$$t \equiv \frac{E_R^{(0)}}{-E_I^{(0)}} = \frac{E_R^{(0)}}{E_S^{(0)}} \frac{E_S^{(0)}}{-E_I^{(0)}} = -\frac{1}{2}\frac{y}{x} .$$

This parameter is a measure of the disruptive centrifugal force compared to the gravitational cohesion. (It is half the tangent of the angle to a point x,y in the $x - y$ plane, measured clockwise from the negative x-axis.)

As you know a gravitating mass with small angular momentum (small t) assumes the shape of an oblate spheroid (the Maclaurin spheroid). Such a spheroid remains a shape of equilibrium for all values of t, flattening more and more towards a thin disc as t tends to infinity. In 1834 Jacobi made the startling discovery that if the angular momentum exceeds a certain critical value ($t > 0.192$) a triaxial ellipsoid is also a configuration of equilibrium, and in fact secular stability passes from the Maclaurin to the Jacobi shapes. Towards the end of the last century Poincaré showed that as one moves along the Jacobi sequence of ellipsoids, other distinct families of equilibrium shapes bifurcate at definite values of the angular momentum. The first such crossing occurs at $t = 0.316$. For values of t

less than 0.316 there exist, in addition to the Maclaurin and Jacobi ellipsoids, also reflection-asymmetric ("pear-shaped") figures of equilibrium. At $t = 0.486$ another crossing occurs, this time by a reflection symmetric family. For $t > 0.486$ these shapes have the appearance of a Jacobi ellipsoid modified by a necking or waist in the middle, and for $t < 0.486$ they look like a Jacobi ellipsoid with a bulge in the middle and two neckings on either side. (One might give Paul Appell's name to this family.) Further such crossings at $t = 0.903$, 1.161, etc. correspond to higher ellipsoidal harmonic ripples on the basic Jacobi figure. (I have called them Humbert and Orlov families, respectively, after two mathematicians who contributed to locating their bifurcation points).

Figure 16 summarizes the behavior of these families in the usual way by plotting the semi-major axis as a function of t. Also shown in Fig. 16 is a further family of equilibrium shapes, the system of two equal fragments rotating about their common center of mass (Darwin's binary "star" system). In this configuration of equilibrium each half has to a good approximation the shape of a triaxial ellipsoid. The length of the whole figure goes to infinity with increasing angular momentum. With decreasing angular momentum the two "stars" approach each other and, finally, as the centrifugal force becomes too weak to support the increasing gravitational attraction, the family of Darwin's binaries comes to an end around $t = 0.484$. Combining some of Jeans' early speculations with our own more recent studies, I have sketched in (as a dashed curve) the probable fate of this family. After bending out at $t = 0.484$ it probably bends back again at $t \approx 0.65$ (this value is not known accurately), to join the dumb-bell-like Appell family of shapes! We anticipate a similar connection between the Orlov family and a three-star family (a system of three colinear fragments with reflection symmetry rotating about the common center of mass).

The most important feature of Fig. 16 is the critical value $t = 0.316$, where the Poincaré pears bifurcate. Its physical significance is that beyond this value the Jacobi ellipsoids are unstable and any additional angular momentum would make them disintegrate. A lot has been written in the past 100 years about the question what a Jacobi shape would disintegrate into, and the question remains unanswered. There are two aspects of the problem that have not been stressed, as far as I know, but which seem obvious when you exploit the analogy of this problem to the phenomenon of nuclear fission. The first is that the Poincaré pears are saddle-point shapes in the same sense that the Bohr-Wheeler dumb-bells are saddle-point shapes, i.e., they both determine the barrier against disintegration for a system that has not yet reached the limit of stability (which limit is given by $x = 1$ in the nuclear case and $t = 0.316$ in the gravitating case). From this point of view it is strange that the Poincaré pears have received so little attention once it was found they were unstable. In the nuclear case, you will remember, the tracing out of the unstable Bohr-Wheeler saddles was the outstanding problem of fission theory. By contrast, in the gravitational case, we still don't know what happens to the Poincaré pears as t is decreased below 0.316! This is a fascinating riddle. It seems rather certain that for $t = 0$ the Poincaré pears no longer exist, so where and how did they disappear?

The second neglected aspect of the question how the Jacobi ellipsoids might disintegrate is what lies beyond the Poincaré saddle-point pass? In particular, what is the absolute minimum in the effective potential energy towards which the disintegrating Jacobi ellipsoid is presumably drawn after overcoming the saddle pass in the barrier against disintegration? In the nuclear case the absolute minimum in the energy is n equal fragments at infinity, the optimum value of n depending on the value of x (approximately $n_{opt} \approx 4x$). In the gravitational case it does not seem ever to have been stated clearly what the absolute minimum in the effective potential corresponds to. The answer is pathological but instructive. Thus in order to reduce E in Eq. (1) to its lowest possible value (in the case of negative x) one should divide the total mass into one large spherical part and one very small part (a "satellite"), and place the small part so far away that, despite its smallness, the moment of inertia of the whole figure is very large. By making the size of the satellite tend to zero but its distance tend to infinity sufficiently rapidly one can make the moment of inertia tend to infinity, and thus make the rotational energy vanish. One thus arrives at a configuration whose gravitational and surface energies are no greater than those of a single sphere, but whose rotational energy has been reduced to zero by the artifice of making the satellite carry all the angular momentum at a vanishingly small rate of rotation.

This simple observation, that the absolute minimum in the effective potential corresponds to a very asymmetric configuration of a small satellite at infinity, may be the basic reason why the Jacobi ellipsoid becomes unstable with respect to an asymmetric (pear-shaped) deformation. This asymmetry, which makes one tip of the ellipsoid more pointed (and the other less) may be an expression of the underlying urge of the rotating figure to emit a small satellite and send it off to infinity. This speculation also suggests a solution to the riddle of what happens to the Poincaré pear as t is decreased below 0.316. My guess is that as the tip of the Pear becomes more elongated with decreasing t it eventually reaches out to the "neutral point" in the potential surrounding the pear (the neutral point in the sum of the gravitational and centrifugal potentials). Such neutral points are always outside the surface of a Maclaurin or Jacobi ellipsoid, but for the Pear there is no reason why the elongating tip should not touch the neutral point. Physically this means that at the tip the centrifugal force has overcome the gravitational attraction and matter begins to stream out from it. (An analogous streaming occurs when a dielectric drop is put between the plates of a condenser, and the electric field increased. The drop stretches at first into an elongated pseudospheroid, but at a critical field the tips sharpen up and begin to emit a stream of droplets. See also Ref. 6.)

A further thought which is suggested by these considerations is that, in general, the configuration of an infinitesimal satellite placed at the neutral point (or the lowest neutral point, if there are several) i.e., a satellite in synchronous orbit around the central body, is a configuration of equilibrium whose formal significance is that of a saddle-point pass that must be overcome when converting a given rotating configuration of equilibrium into the absolute minimum configuration of a sphere and a satellite at infinity. Thus, in addition to all the families of equilibrium mentioned so far, there is a matching set of "Ghost Families", identical to the basic set but with an infinitesimal satellite (or satellites) in a synchronous orbit.

Figure 17 is an attempt to summarize these speculations. The maximum radius vector (tip-distance) of the Ghost Families is the radius of the synchronous orbit and thus the Maclaurin and Jacobi Ghosts are shown as dashed curves above the conventional families. In the case of the Poincaré pear the elongating tip meets its Ghost in a typical limiting point (when the tip touches the synchronous satellite), with the result that no Poincaré pears exist below some critical value of t, yet to be determined. Similar turning points probably mark the limits, on the left, of the Appell, Humbert and Orlov families as their tips touch the relevant neutral points.

7. THE LIMIT $x^{-1} \to 0$. THE BROKEN SYMMETRY HYPOTHESIS

A puzzle arose in trying to fit together the case of large negative x and the astronomical case of $x^{-1} = 0$. Thus for large but finite negative x values our calculations indicated that the rotating triaxial Beringer-Knox pseudo-ellipsoids come to an end at a finite value of the angular momentum, given by y_{II}, which corresponds to a limiting t of about 0.6-0.7. But in the astronomical case the Jacobi ellipsoids are known to continue on to infinite values of t. What then happens between x^{-1} small, and x^{-1} zero, i.e., what is the difference between the case of a finite surface energy, however small, and no surface energy? I think the answer is as sketched in Fig. 18. In the case of no surface energy the Jacobi and Appell families cross (at $t = 0.486$), as discussed in Sec. 5. When the surface energy is switched on the crossing is, I believe, broken, and the Jacobi-like shapes continue on to become the Appell symmetric dumb-bells, whereas the double-waisted Appell figures merge into what used to be the Jacobi shapes beyond the crossing. Formally such a breaking of the crossing between families of solutions is well-known, for example in atomic or nuclear spectroscopy. Crossings (of eigenvalues) are in fact the exception rather than the rule and are only possible if special symmetries are satisfied. I believe the analogy carries through to the present situation. (In both cases the formal problem is the diagonalization of a secular determinant.) It is only because of the special symmetry (in a generalized sense) of the pure inverse-distance problem (which also results in pure ellipsoids being exact solutions) that a crossing between two families like the Appell and Jacobi shapes is possible. The addition of the slightest amount of surface energy breaks this symmetry and the families no longer cross. From this point of view the astronomical case, which had been studied for centuries, is an <u>atypical</u> situation, and a study of the case with surface tension is important, among other things, in restoring the proper perspective on the general problem.

With the above hypothesis it is possible to connect the case with surface tension with the astronomical case in a way indicated in Fig. 19. The continuation to minus infinity of the critical curve $y_{II}(x)$ in Fig. 6, where the Beringer-Knox shapes bend back into the Pik-Pichak shapes (see Fig. 14) corresponds to the critical value $t \approx 0.65$, where the Appell shapes bend down to become the Darwin-Jeans shapes. (Fig. 16) The second bend in Fig. 16 at $t = 0.484$, where the Darwin-Jeans shapes become the Darwin binaries, may be traced to finite values of x and is indicated as the critical curve y_{IV} in Fig. 6.

The continuation to minus infinity of the dashed part of the curve $y_{III}(x)$ in Fig. 6, where the Beringer-Knox shapes lose stability against asymmetry, corresponds to the critical value $t = 0.316$, where the Jacobi shapes lose stability against a pear-shaped deformation. According to our broken symmetry hypothesis there is no critical curve for finite values of x corresponding to the crossing at $t = 0.486$ of the Jacobi and Appell families. On the other hand, one is led to the prediction (quite unexpected unless one is aware of the astronomical limit) that in the case of finite (negative) x there must exist further families of equilibrium shapes beyond the limiting angular momentum y_{II}. These families would correspond to the astronomical Jacobi family and its bifurcations, but with the crossings at even harmonic bifurcations (Appell, Orlov etc.) broken according to the scheme of Fig. 18. The fate of these families as the surface tension increases is completely unknown.

8. LOOSE ENDS

I have already mentioned several questions and puzzles that have not been answered satisfactorily. I should also say that many of the results I quoted are only approximate and in some cases quite uncertain. In addition there is a whole list of families of equilibrium shapes that I have not even mentioned, some of which have been studied to a limited extent. Let me make a partial list:

1. Equilibrium shapes for $y < 0$.
2. Equilibrium shapes in the form of spherical harmonic distoritions of a sphere, which cross the spherical family as x increased beyond 1. (These crossings are like the infinitely many Poincaré crossings of the Jacobi ellipsoids.)
3. Families of multiply-necked cylinders which for $y = 0$, $x \to 0$ tend to strings of equal spheres in contact. Branchings from these families that occur as x increases.
4. Families which for $y = 0$, $x \to 0$ tend to other arrangements of equal spheres (triangular, tetrahedral, etc.).
5. Thick-walled spherical shells (nuclear bubbles); a pair of such configurations appears when x exceeds 2.0216.
6. Unequal spherical fragments at infinity.

The list could be extended indefinitely.

CONCLUSION

I hope that I have succeeded in giving you an impression of the richness of the problem defined so innocently as the search for equilibrium shapes of a rotating mass. Even in the nuclear case with no rotation one is drawn by stages from thinking of a single sphere as the solution, to the inclusion of many equal fragments at infinity as formal solutions, and then through topological arguments to the realization that there must also be dumb-bells with equal or unequal bulbs and many other families as well. With rotation included the mathematical structure acquires baroque ramifications. One of the joys of disentangling this structure has been the unification of the astronomical, hydrostatic and nuclear problems, and the insights gained by confronting the different fields.

Let me end by stressing that the problem of the equilibrium configurations of a rotating drop or bubble with inverse-distance interactions defines a beautiful mathematical structure which has been only partially explored. Even gross qualitative questions remain unanswered, and there is a serious lack of quantitative results.

REFERENCES

1. J. R. Nix, Nucl. Phys. A130, 241 (1969) and Los Alamos report LA-DC-72-769, Aug. 15, 1972.

2. S. Chandrasekhar, "Ellipsoidal Figures of Equilibrium", Yale University Press, 1969.

3. P. Appell, "Traité de Mécanique Rationnelle", Gauthier-Villars, Vol. 4, Paris, 1932.

4. S. Cohen, F. Plasil, and W. J. Swiatecki, Annals of Physics 82, 557 (1974).

5. J. R. Nix and W. J. Swiatecki, Nucl. Phys. 71, 1 (1965).

6. G. I. Taylor, Proc. Roy. Soc. A280, 383 (1964).

FIGURE CAPTIONS

1. The planet Jupiter.

2. A solidified glass droplet, about 1 mm in length, from the lunar soil.

3. Sketches made by Niels Bohr during a conversation on the liquid drop theory of nuclear fission and (on the right) shapes of a fissioning Np^{237} nucleus calculated by J. R. Nix according to that model.

4. Various physical systems arranged according to the x and y parameters specifying the intensities of inverse-distance and rotational energies relative to the surface energy.

5. A schematic potential energy surface illustrating a metastable hollow A, the absolute minimum C, a saddle-point B and a mountain top D.

6. Stability properties of various systems in the x-y parameter plane.

7. Schematic potential energy map for a nucleus, showing the spherical equilibrium hollow, the two- and three-fragment valleys, the Bohr-Wheeler saddle pass and the Businaro-Gallone mountain tops.

8. Nuclear saddle-point shapes in their dependence on the fissility parameter x.

9. The deformation energy of three heavy nuclei with fissility parameters 0.6, 0.8, and 1.0. At $x = 1.0$ the fission barrier vanishes.

10. The major and minor semi-axes of the Bohr-Wheeler saddle shapes in their dependence on the fissility parameter x. The dashed curves give the semi-axes of the Businaro-Gallone shapes.

11. The mass decrements (related to binding energies) of nuclei and the fit obtained by means of the liquid drop model.

12. The lower part shows the deviations of the ground state masses of heavy nuclei from a liquid drop model fit. The upper part compares the experimental and calculated masses for the same nuclei deformed into their saddle-point configurations.

13. Axially symmetric equilibrium shapes for uncharged (Plateau) globes as function of the rotation parameter y. (The axis of symmetry is vertical.)

14. Major semi-axis for Hiskes oblate shapes, Beringer-Knox triaxial shapes, and Pik-Pichak saddles as functions of y, for $x = 0.3$.

15. Ground states (heavier lines) and saddle shapes (lighter lines) for $x = 0$ and $x = 0.3$ and various values of y. In all figures H refers to "Hiskes", BK to "Beringer-Knox" and PP to "Pik-Pichak". Hiskes shapes have axial symmetry about the axis of rotation (vertical axis). The Beringer-Knox and Pik-Pichak shapes shown have approximate symmetry about the horizontal axis and only a mean transverse section is displayed for these shapes. (For $x = 0$, $y = 0$ the saddle shape is two spheres in contact.)

16. Major semi-axis for astronomical families of shapes.

17. Speculative (and schematic) extension of Fig. 16 to indicate the probable relation of the known equilibrium families to their "ghosts" (configurations with an infinitesimal satellite in synchronous orbit).

18. Illustration of the breaking of crossings between equilibrium families associated with a symmetry-breaking force, such as the surface tension.

19. The fitting together of the nuclear and astronomical domains in the x-y plane.

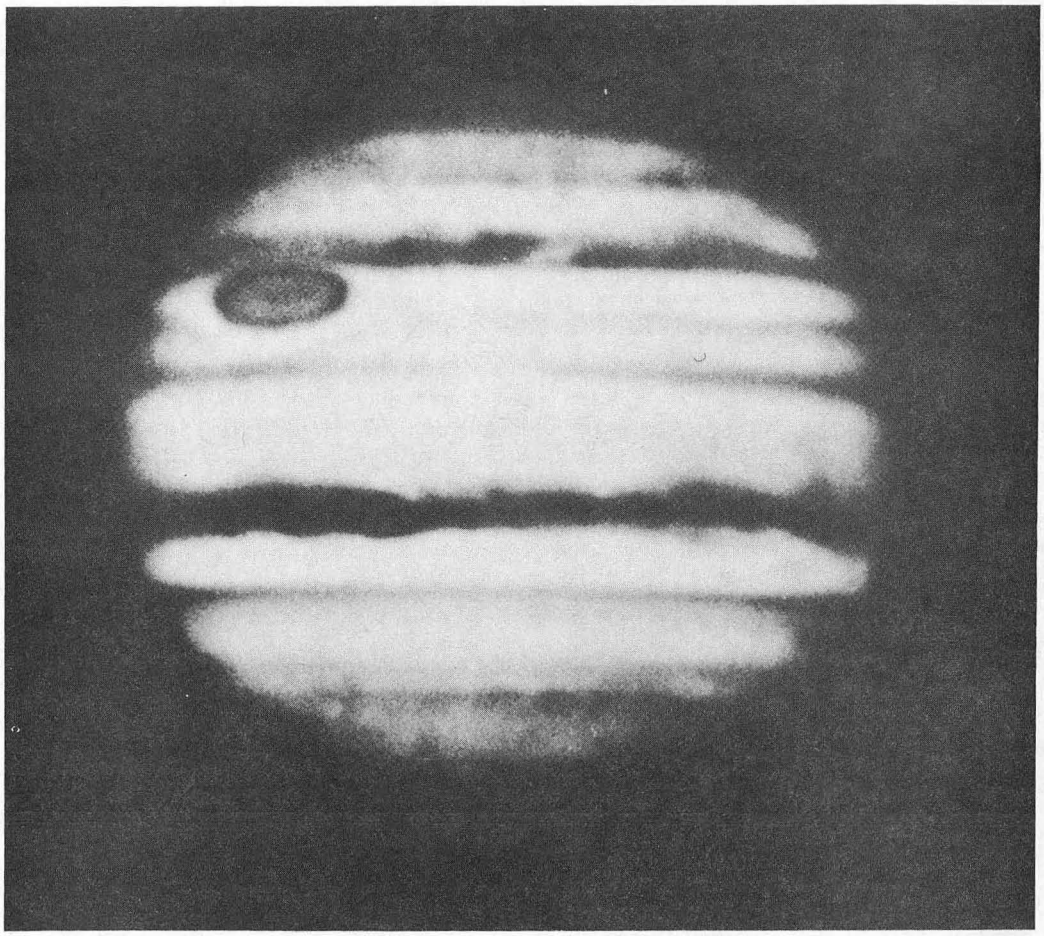

Fig. 1

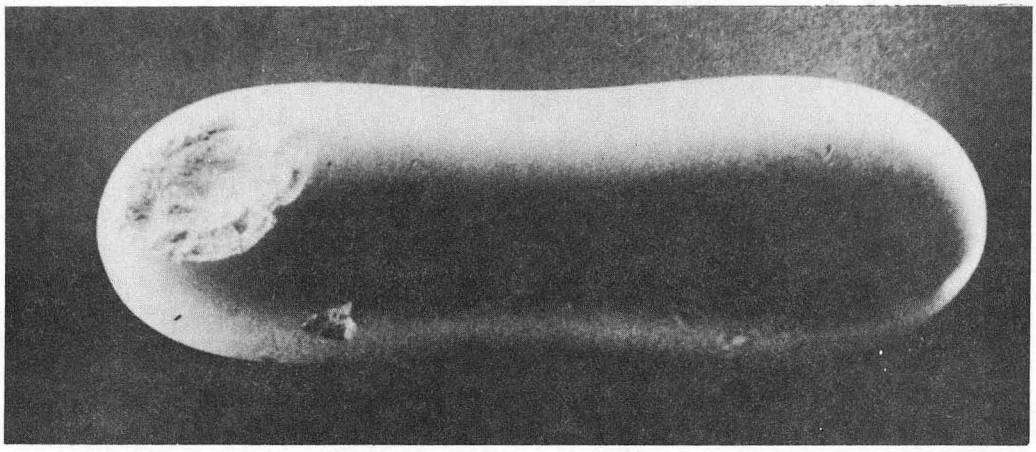

Fig. 2

XBB 7410-7058

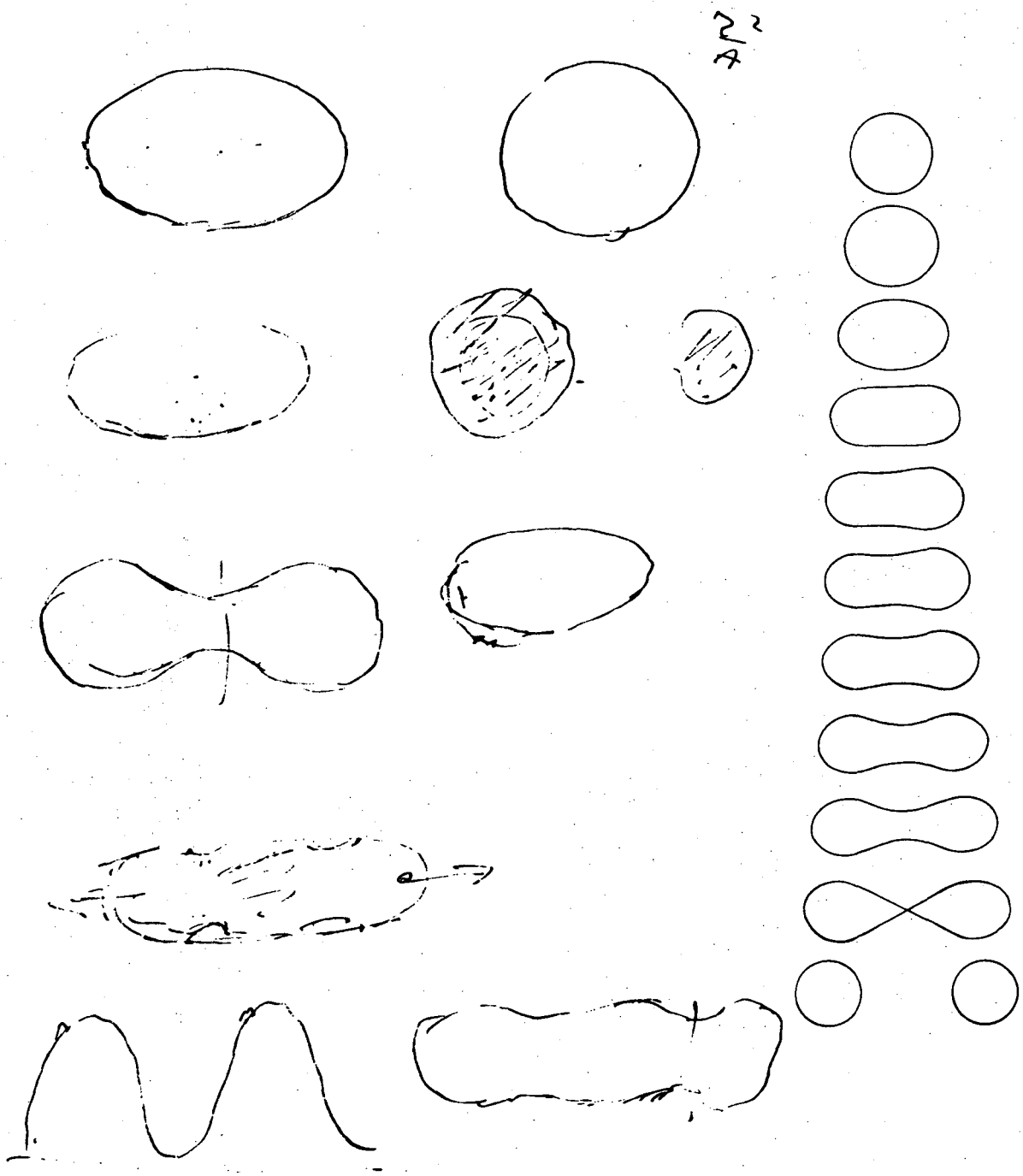

Kierowca samochodu z Bohrem (7.10.1950 – jego urodziny). Temat: niesymetryczny rozpad jądra.

XBL 7410–1883

Fig. 3

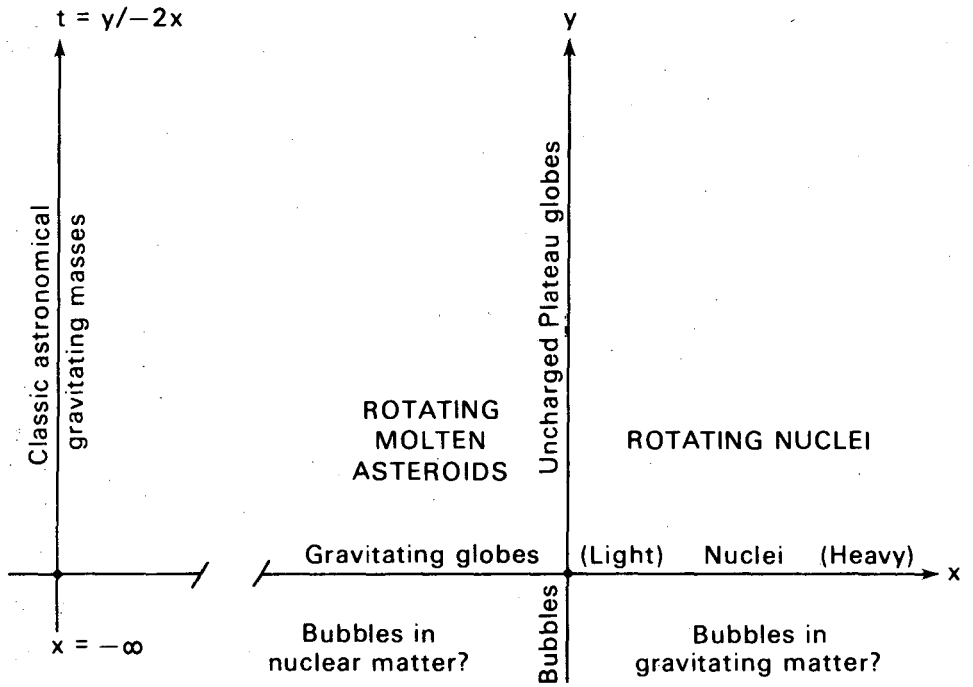

Fig. 4

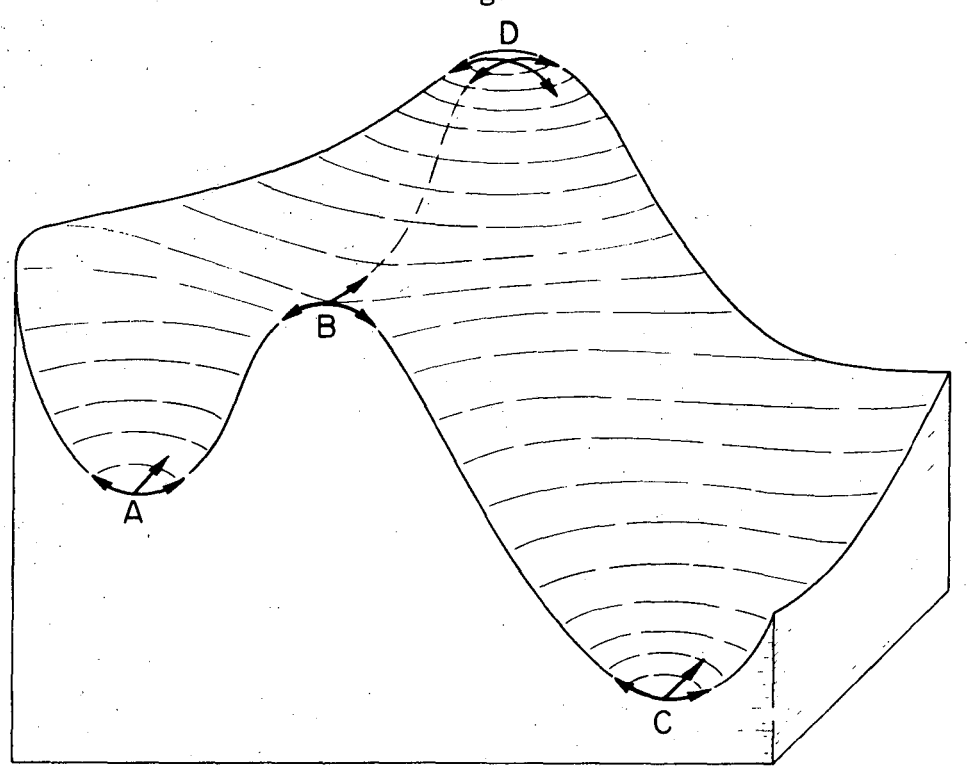

XBL 7410–1993

Fig. 5

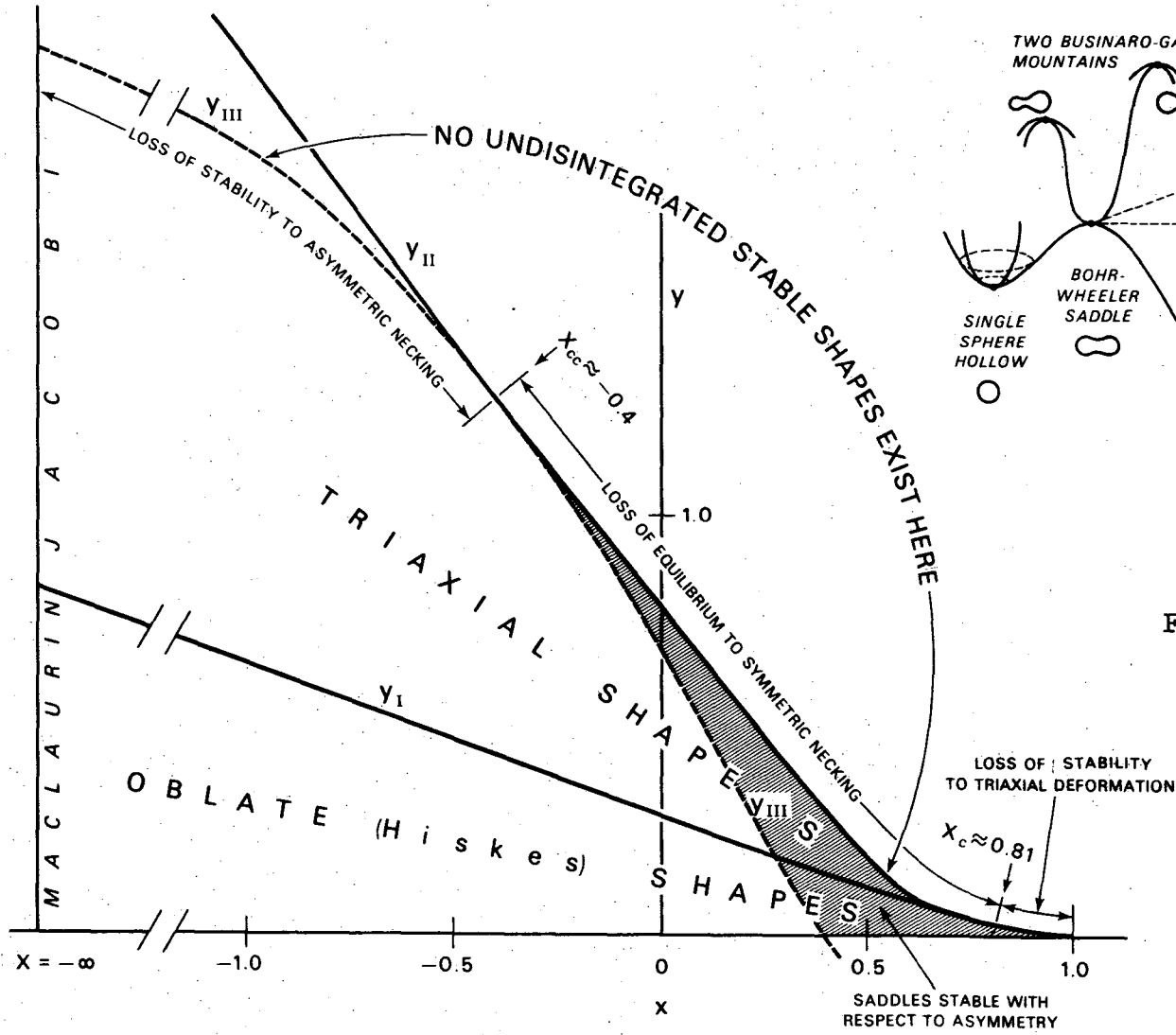

Fig. 6

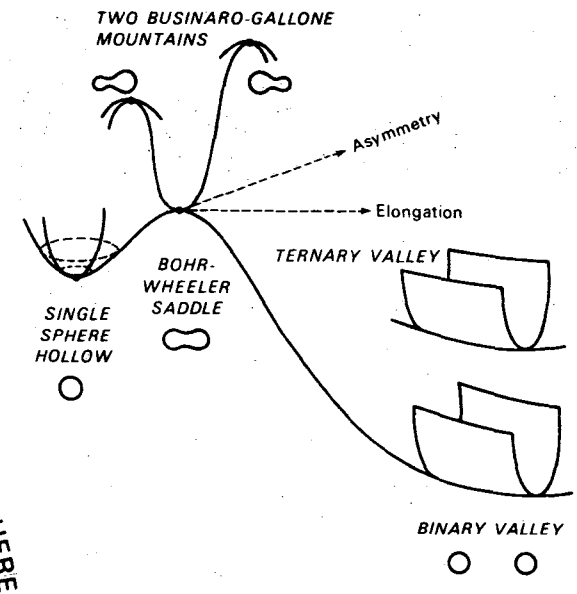

Fig. 7

XBL 7410–1992

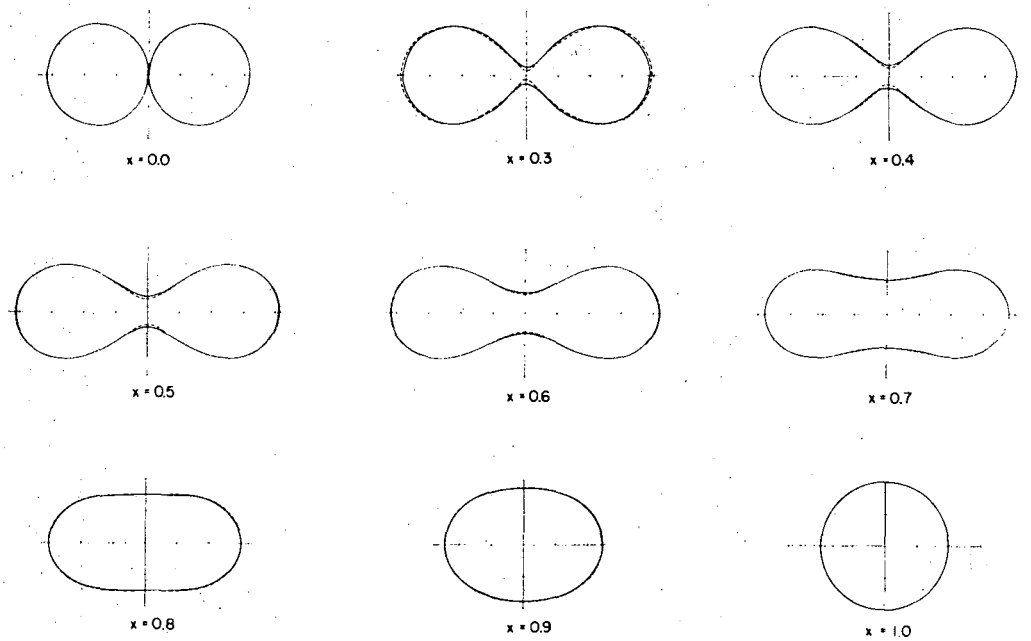

Fig. 8

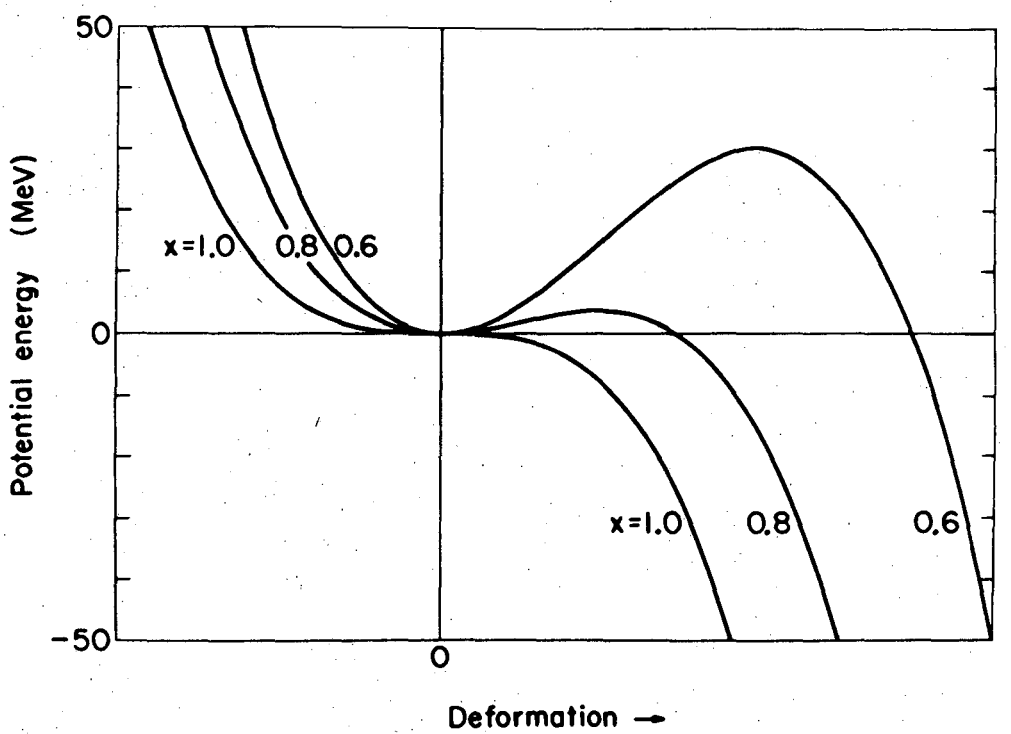

XBL 7410–1937

Fig. 9

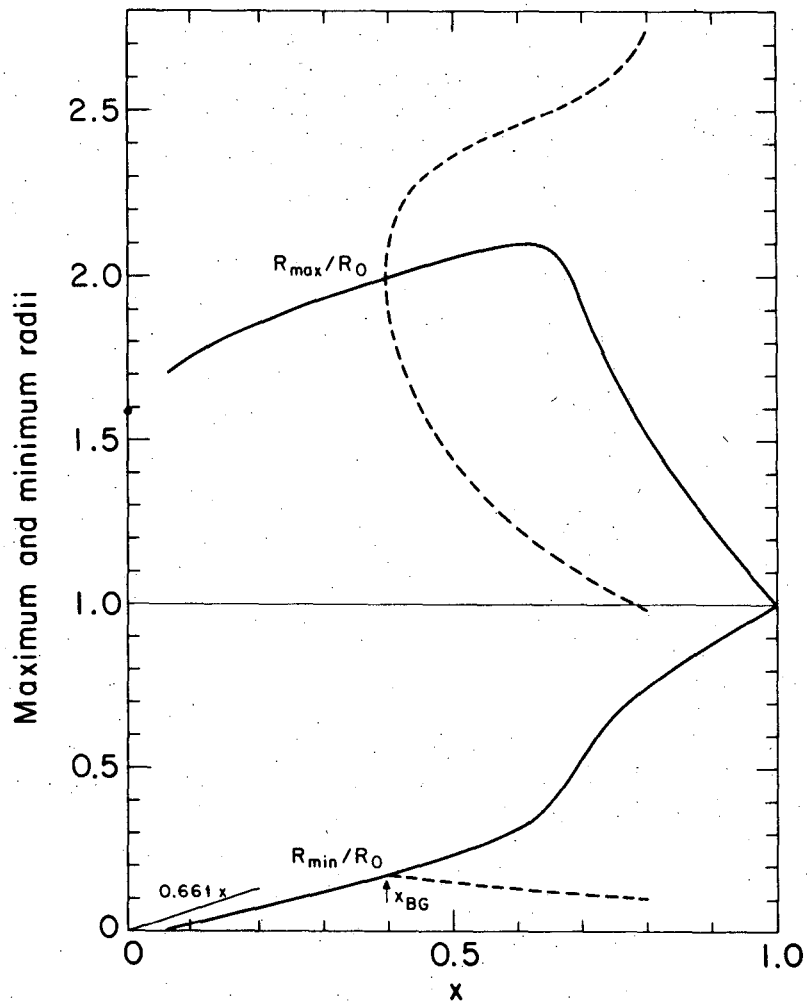

Fig. 10

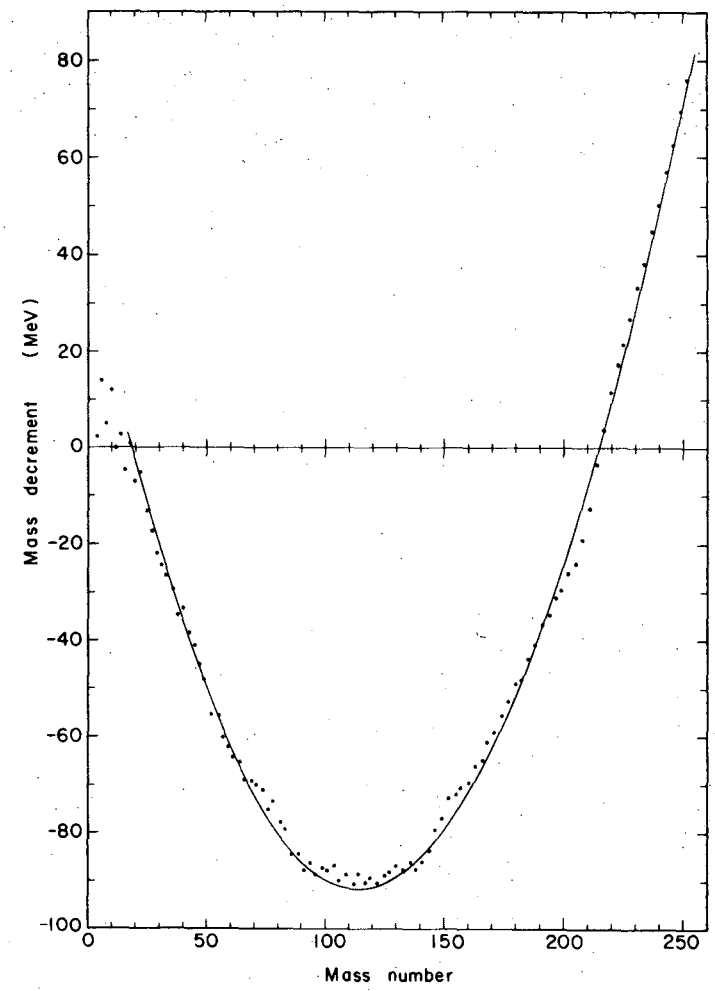

XBL 7410–1935

Fig. 11

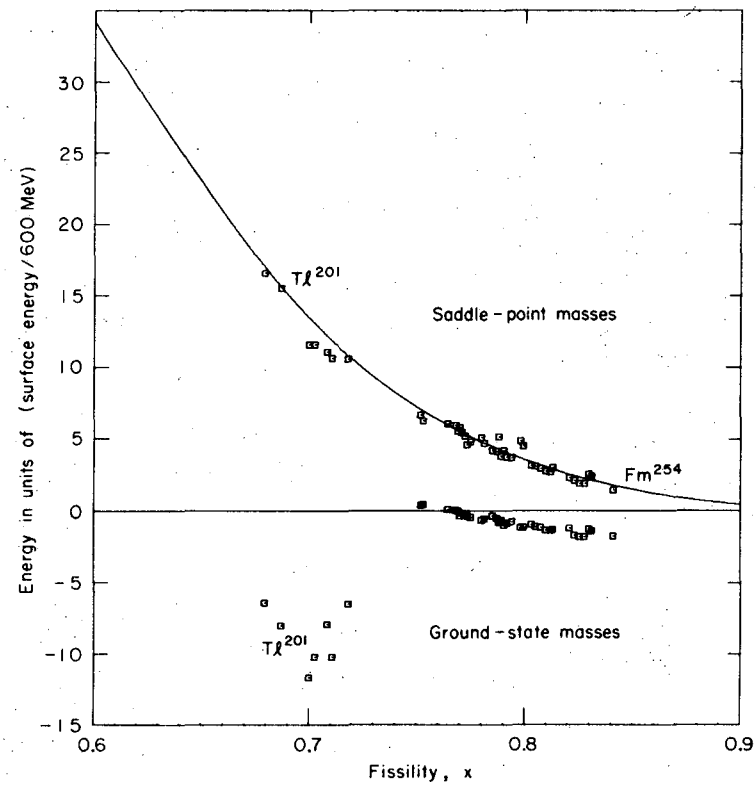

Fig. 12

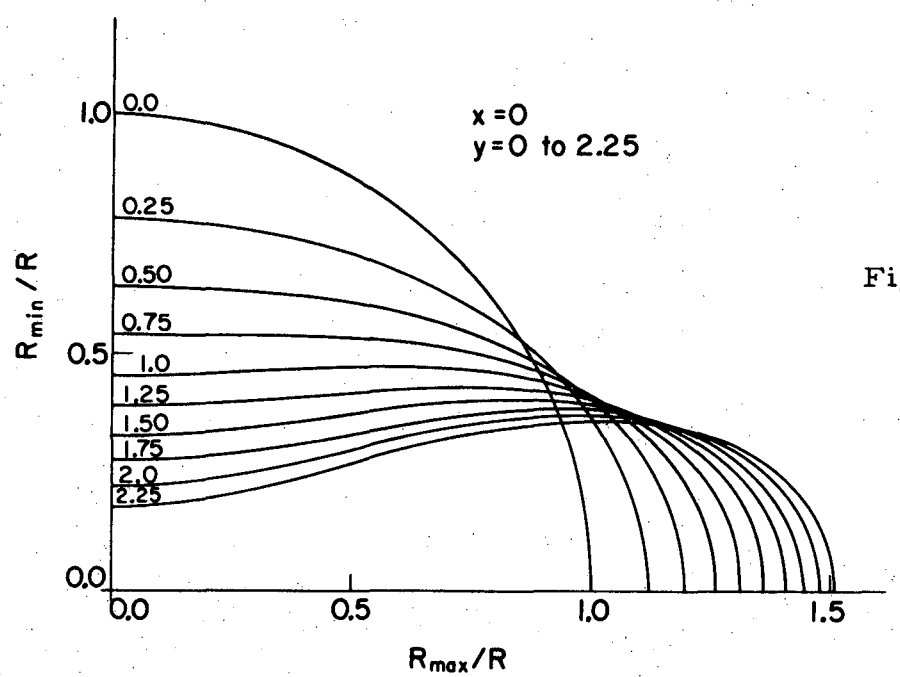

Fig. 13

XBL 7410—1936

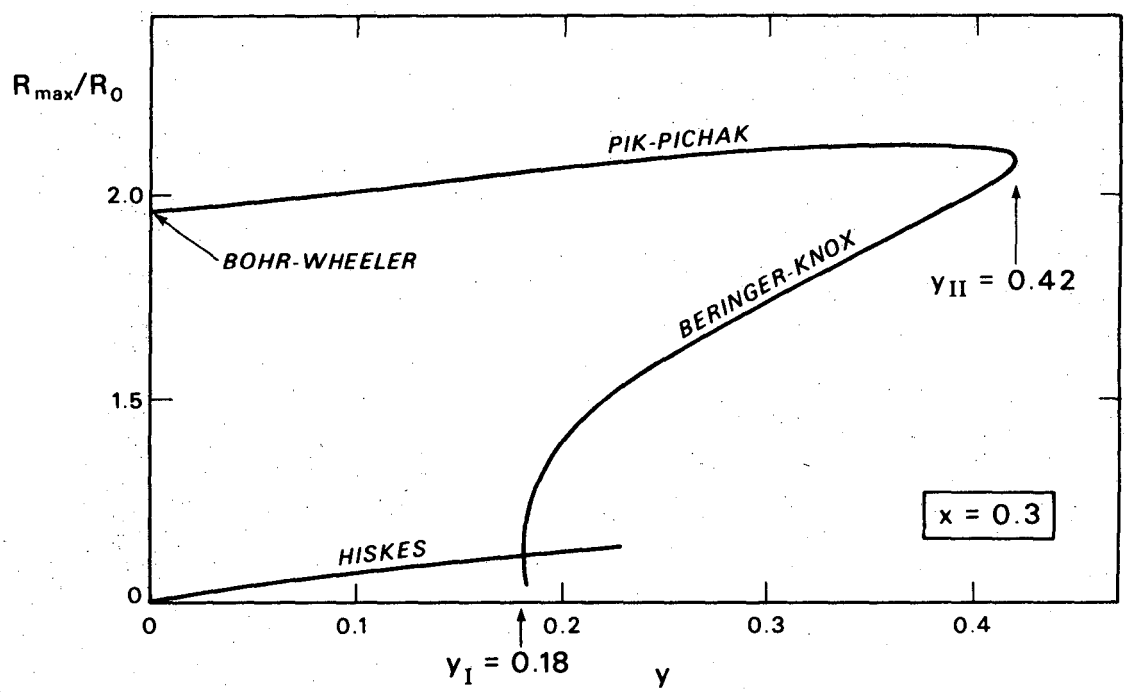

Fig. 14

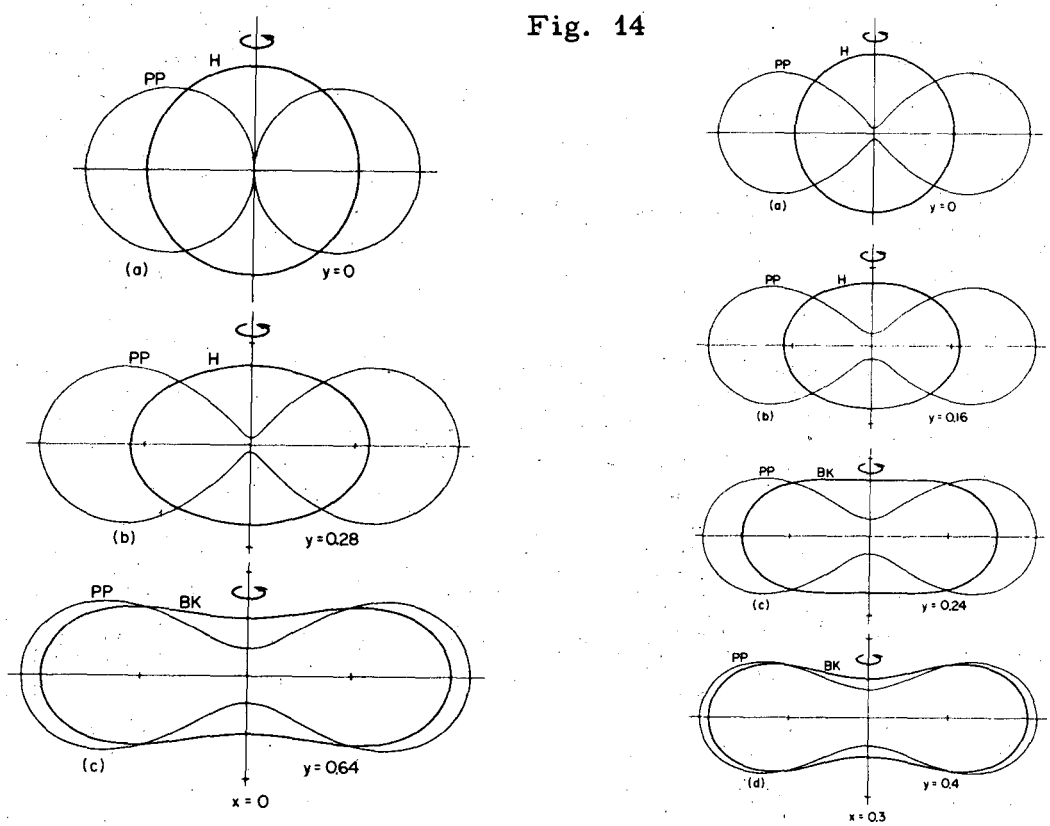

XBL 7410–1996

Fig. 15

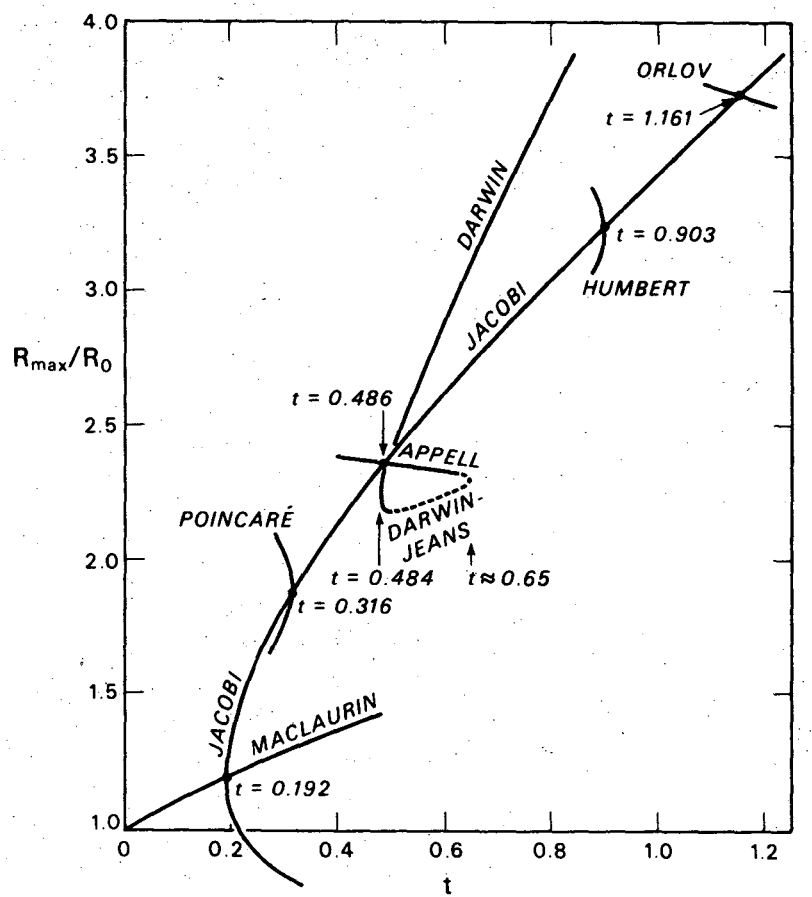

Fig. 16

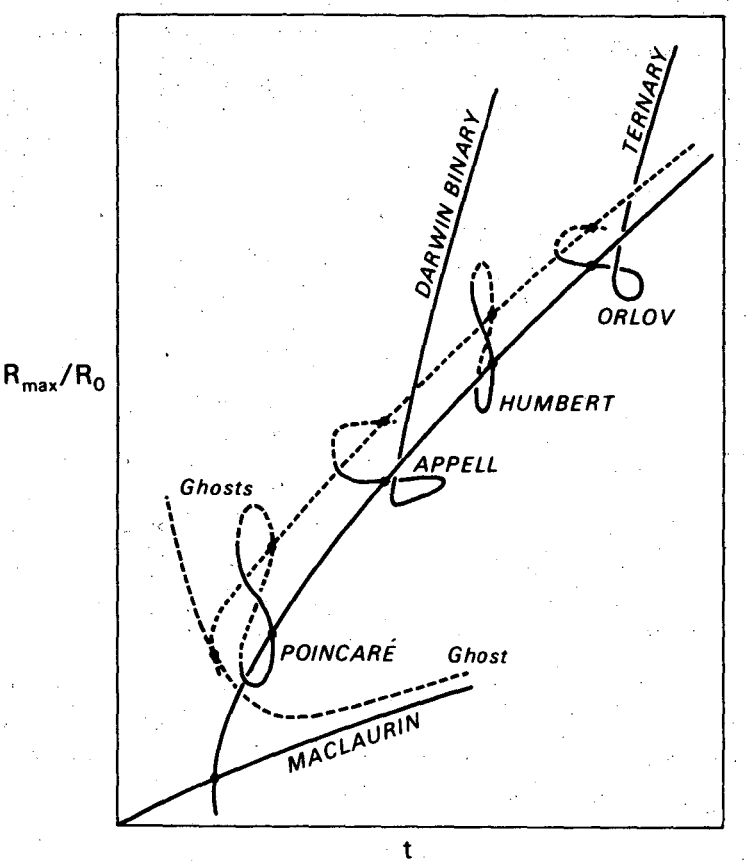

XBL 7410–1994

Fig. 17

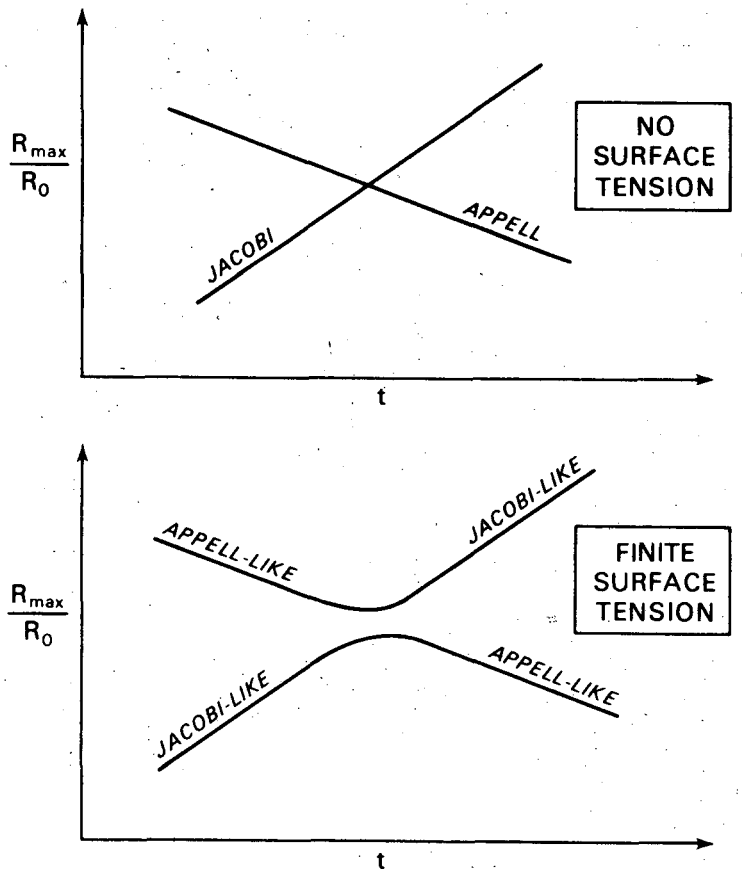

Fig. 18

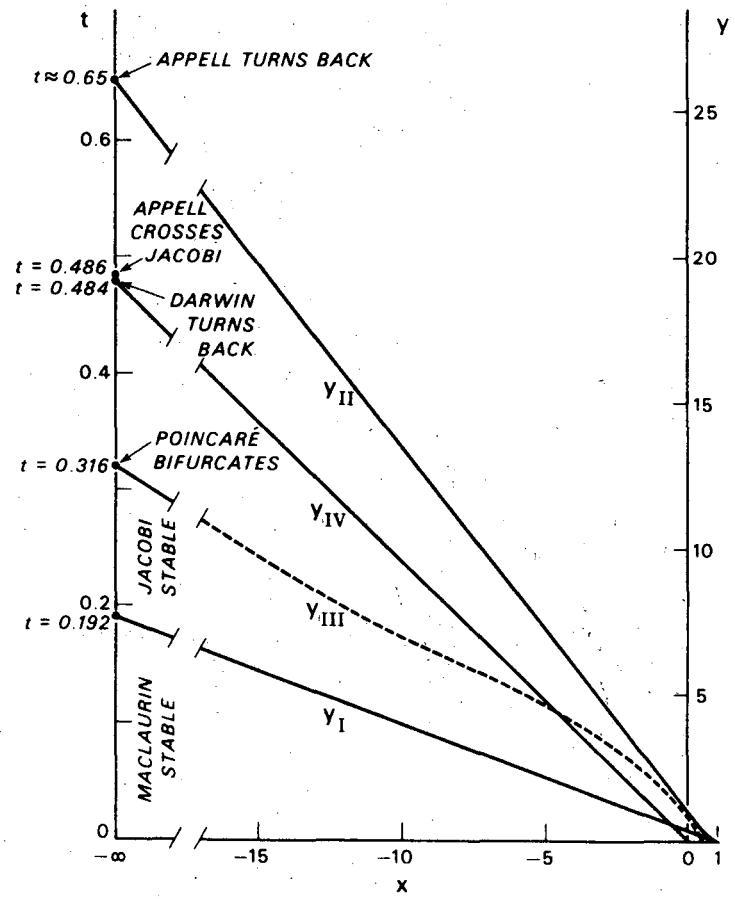

XBL 7410–1995

Fig. 19

LEGAL NOTICE

This report was prepared as an account of work sponsored by the United States Government. Neither the United States nor the United States Atomic Energy Commission, nor any of their employees, nor any of their contractors, subcontractors, or their employees, makes any warranty, express or implied, or assumes any legal liability or responsibility for the accuracy, completeness or usefulness of any information, apparatus, product or process disclosed, or represents that its use would not infringe privately owned rights.

TECHNICAL INFORMATION DIVISION
LAWRENCE BERKELEY LABORATORY
UNIVERSITY OF CALIFORNIA
BERKELEY, CALIFORNIA 94720